

Copper and/or cobalt modified nanostructured Ce-Zr mixed oxides as efficient catalysts for ethyl acetate total oxidation

R. N. Ivanova^{1*}, M. D. Dimitrov¹, D. G. Kovatcheva², T. S. Tsoncheva¹

¹ Institute of Organic Chemistry with Centre of Phytochemistry, Bulgarian Academy of Sciences, 1113 Sofia, Bulgaria,

² Institute of General and Inorganic Chemistry, Bulgarian Academy of Sciences, 1113 Sofia, Bulgaria

Received, 13 April 2017; Revised, 15 May 2017

Dedicated to Acad. Ivan Juchnovski on the occasion of his 80th birthday

By using an original approach combining the utilization of urea as a precipitator followed by hydrothermal treatment were obtained nanostructured Ce-Zr mixed oxides (Ce/Zr = 3:7 or 5:5). The obtained oxides were modified with copper and/or cobalt via incipient wetness impregnation from the corresponding metal nitrates. The obtained materials were characterized by X-ray diffraction, nitrogen physisorption, UV-Vis spectroscopy, temperature-programmed reduction (TPR) with hydrogen and their catalytic activity and selectivity in ethyl acetate oxidation was studied as well. The introduction of transition metal oxide within the parent Ce-Zr oxides decreases the start of the conversion with up to 50 K, increases substantially of the catalytic activity within the 550-650 K range and facilitates the selectivity to total oxidation of ethyl acetate. The influence of the type of modifying transition metal is better distinguished for the 3Ce7Zr support, especially within 550-600 K range, showing that the addition of copper only is sufficient for achieving the best catalytic results. At the same time, the support with higher ceria amount (5Ce5Zr) favors the catalytic behavior of the cobalt-containing modifications as well due to enhanced Co-Ce interaction.

Key words: CeO₂-ZrO₂ mixed oxides; cobalt and copper oxide modification; ethyl acetate total oxidation

INTRODUCTION

Ceria-zirconia mixed oxides are widely studied due to their excellent redox properties provoked by the formation of Ce_{1-x}Zr_xO₂ solid solution [1-3]. In our previous studies we have shown the potential of ceria-zirconia mixed oxides in ethyl acetate total oxidation [4,5]. The ethyl acetate oxidation is known as two-step process including dehydration to ethanol and acetic acid on acidic sites and their further oxidation with lattice oxygen following Mars-van-Krevelen mechanism [6,7]. Depending on the efficiency of the catalysts, several by-products, such as ethanol, acetaldehyde and acetic acid could be produced. We demonstrated that the selectivity to CO₂ on ceria-zirconia oxides was not satisfactory below 600-650 K, nevertheless the variations in the samples composition and the preparation procedure used [4,5]. The formation of ceria-zirconia solid solution in the nanoscale could provide more active oxygen species and further enhance the overall redox capability [8]. Another important advantage of the nanostructured metal oxides due to their well developed specific surface area is the facilitated introduction within them of another metal/metal oxide component in highly

dispersed state [9]. The introduction of readily reducible transition metal oxide could further improve the catalyst redox function. Copper and cobalt have favorable effect on the redox properties of both ceria and zirconia not only as monocomponent- [10-13] but as bicomponent [14-18] support systems as well. The aim of the present paper is to show the perspective of using nanostructured transition metal oxides in the design of multicomponent nanocomposite materials with potential application as efficient catalytic systems for total oxidation of ethyl acetate as representative of volatile organic compounds. For this purpose, on the basis of previously optimized synthesis procedure in the absence of long-chain organic template [4], Ce-Zr mesoporous oxides with optimal Ce/Zr ratio (Ce/Zr=5:5 or 3:7) were used as supports for the introduction and stabilization of copper and/or cobalt oxides nanoparticles.

EXPERIMENTAL

Materials

Two nanostructured Ce-Zr mixed oxides with various metal ratio (3:7 and 5:5) were synthesized using precipitation technique from the corresponding metal chlorides and in absence of long-chain surfactant followed by hydrothermal

* To whom all correspondence should be sent:
E-mail: radostinaiv@abv.bg

treatment step at 373 K according to a procedure reported previously [4]. The obtained Ce-Zr samples are calcined at 573 K and afterwards were modified with copper and/or cobalt by incipient wetness impregnation technique from the corresponding metal nitrates aqueous solutions. The total amount of copper and/or cobalt in the obtained multicomponent nanocomposites is 8 wt. %. The samples are designated as follows: $x\text{Cu}_y\text{Co}_z/\text{Ce}_w\text{Zr}$ where x and y correspond to the amount of metal in weight percents, while z/w represents the mol ratio between Ce and Zr. For comparison data for the analogous pure ceria-zirconia nanocomposites calcined either at 573 K (samples 3Ce7Zr and 5Ce5Zr) or at 773 K (samples 3Ce7Zr(773) and 5Ce5Zr(773)) are presented as well.

Methods of characterization

Nitrogen sorption measurements were recorded on a Quantachrome NOVA 1200e instrument at 77 K. Before the measurements the samples were evacuated at 423 K overnight under vacuum. The pore size distribution was calculated using a microscopic model, i.e. the non-local density functional theory NLDFT. The crystallinity of the samples was investigated by powder X-ray diffraction (PXRD) measurements performed on Bruker D8 Advance diffractometer equipped with Cu K α radiation and LynxEye detector. The size of the crystalline domains in the samples was determined using Topas 4.2 software with Rietveld quantification refinement. The UV-Vis spectra were recorded on a Jasco V-650 UV-Vis spectrophotometer equipped with a diffuse reflectance unit. The TPR/TG (temperature-programmed reduction/ thermogravimetric) analyses were performed in a Setaram TG92 instrument. Typically, 40 mg of the sample were placed in a microbalance crucible and heated in a

flow of 50 vol. % H₂ in Ar (100 cm³min⁻¹) up to 773 K at 5 Kmin⁻¹ and a final hold-up of 1 h. The catalytic experiments were performed in a flow type reactor (0.030 g of catalyst) with a mixture of ethyl acetate (1.21 mol %) in air with WHSV – 335 h⁻¹. Gas chromatographic (GC) analyses were carried out on HP5850 apparatus using carbon-based calibration. The samples were pretreated in Ar at 423 K for 1 h and then the temperature was raised with a rate of 2 K/min in the range of 423–773 K.

RESULTS AND DISCUSSION

Some physicochemical characteristics of the obtained samples are presented in Table 1. Nitrogen physisorption measurements were conducted in order to elucidate the textural properties of the studied samples (Fig. 1, Table 1). All isotherms are of type IV characteristic of mesoporous materials. Two effects are worth to be mentioned here. First, the modification with copper only leads to a complete loss of microporosity, nevertheless of the support used, which could be a result of preferred copper deposition within the present micropores of the Ce-Zr host leading to its closer contact with the host structure. On the other hand, the extent of microporosity registered within the other modifications is preserved, and even increases in case of 5Ce5Zr host material while in case of 3Ce7Zr support only 6.3 % microporosity is found after its modification within 8Co/Ce3Zr7 sample (Table 1). Besides, almost complete lost of support mesopores with sizes in 2-4 nm range is registered for the bicomponent and pure cobalt modifications (Fig 1, insets). More information about the phase composition and crystallinity of the obtained Ce-Zr hosts and their copper and/or cobalt modifications is found by PXRD technique (Fig. 2).

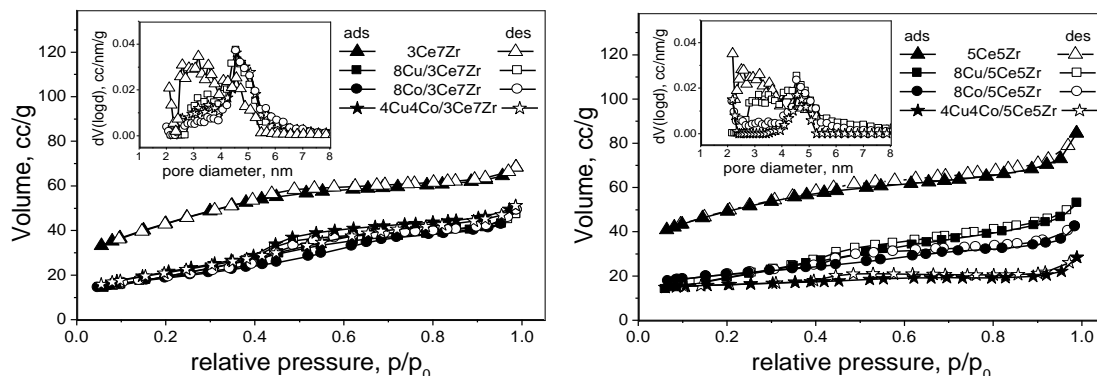


Fig. 1. Nitrogen physisorption isotherms with pore size distributions as insets for the studied pure and mixed metal oxide samples.

Table 1. Some physicochemical characteristics of the studied samples.

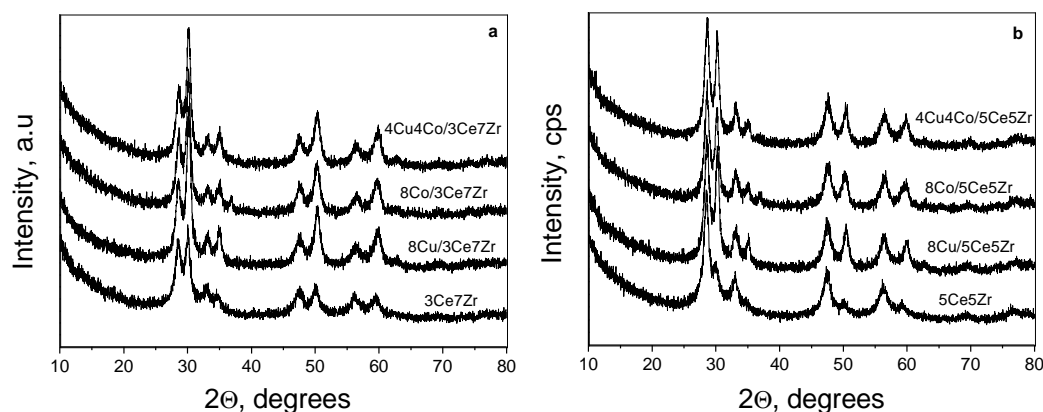
Sample	S_{BET} , m^2/g	V_{total} , cc/g	S_{micro} , m^2/g	V_{micro} , cc/g	Space Group	Unit cell, Å	Crystallite size, nm
3Ce7Zr	154.3	0.11	24.1 (15.6 %)	0.01	Fm-3m	5.424(3)	6
					P4 ₂ /nm	a=3.625(3) c=5.196(6)	9
8Cu/3Ce7Zr	74.0	0.073	-	-	Fm-3m	5.411(2)	8
					P4 ₂ /nm	a=3.615(2) c=5.172(4)	12
4Cu4Co/3Ce7Zr	76.3	0.079	-	-	Fm-3m	5.409(2)	8
					P4 ₂ /nm	a=3.617(2) c=5.185(4)	12
8Co/3Ce7Zr	65.2	0.076	4.1 (6.3 %)*	0.002	Fm-3m	5.407(2)	9
					P4 ₂ /nm	a=3.617(2) c=5.191(4)	13
					Fd-3m	8.088(5)	16
5Ce5Zr	175.9	0.13	72.8 (41.4 %)	0.031	Fm-3m	5.419(2)	7
					P4 ₂ /nm	a=3.603(4) c=5.199(7)	6
8Cu/5Ce5Zr	72.5	0.082	-	-	Fm-3m	5.415(2)	8
					P4 ₂ /nm	a=3.614(1) c=5.157(4)	14
4Cu4Co/5Ce5Zr	59.9	0.044	44.1 (73.6 %)	0.018	Fm-3m	5.409(2)	9
					P4 ₂ /nm	a=3.614(2) c=5.160(4)	15
8Co/5Ce5Zr	75.3	0.066	33.8 (44.9 %)	0.014	Fm-3m	5.402(2)	9
					P4 ₂ /nm	a=3.610(2) c=5.180(4)	14
					Fd-3m	8.073(5)	13

S_{BET} – BET specific surface area; V_{total} – total pore volume; S_{micro} – micropore specific surface area defined by t-plot method; V_{micro} – micropore volume by t-plot method; * in brackets is presented the microporosity of the sample as percentage of S_{BET} .

Both initial supports (5Ce5Zr and 3Ce7Zr) show well-defined reflections of both ceria crystallites with cubic fluorite-like Fm-3m structure and zirconia crystallites with tetragonal P4₂/nm structure and sizes within 6-9 nm range (Fig. 2, Table 1). After the modification, these two phases are preserved, however, the crystallite size increases up to 14-16 nm (Table 1). Besides, only in case of pure cobalt modifications, a new Co₃O₄ spinel phase with cubic Fd-3m structure is

registered as well (Fig. 1) with 13-17 nm crystallite sizes (Table 1). In all other modifications no additional reflections were observed and this is an indication that the copper presence increases the dispersion of the loaded phases nevertheless of the support used.

Uv-Vis analysis has been used to obtain information for the coordination and oxidative state of the present metal ions (Fig. 3).

**Fig. 2.** XRD patterns of the initial and modified Ce-Zr samples.

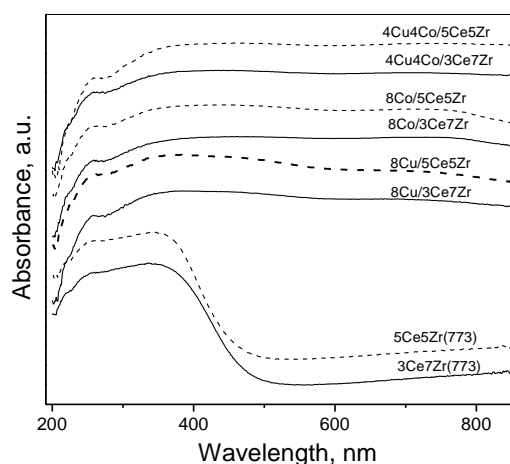


Fig. 3. UV-Vis spectra for the pure ceria-zirconia samples and their modifications

The spectra of both Ce-Zr supports consist of absorption bands characteristic of tetragonal zirconia by the broad feature in their spectra positioned at around 320 nm, while the strong absorption with maximum at about 350–360 nm is ascribed to $O^{2-} \rightarrow Ce^{4+}$ charge transfer (CT) transitions, while that one at about 250 nm – to $O^{2-} \rightarrow Ce^{3+}$ CT transitions (Fig. 3). After the modification these bands are preserved, however, the high absorption registered above 400 nm could be ascribed to the presence of various copper and cobalt oxide species in highly dispersed state. The observed absorption features in the 400–550 and 650–800 nm ranges could be ascribed to either Cu^{2+} ions in finely dispersed CuO crystallites in case of pure copper modifications or to the presence of Co_3O_4 particles within the pure cobalt modifications because of $4T1(F) \rightarrow 4T1(P)$ transitions of octahedrally coordinated Co^{3+} that occur in the former range and the electronic ligand-field $4A2(F) \rightarrow 4T1(P)$ transitions in tetrahedrally coordinated Co^{2+} that occur above 650 nm [19]. This is in agreement with the XRD results where Co_3O_4 spinel phase was found for both 8Co/5Ce5Zr and 8Co/3Ce7Zr samples. In case of the bicomponent modifications, the observed absorption spectra could be interpreted as superposition of the spectra of both pure copper and cobalt modifications, however, the registered very broad bands (Fig. 3) with not well defined maxima do not exclude also the existence of interaction between the individual copper and cobalt oxides.

Additional information for the redox properties of the obtained modifications was obtained by temperature-programmed reduction (TPR) with hydrogen (Fig. 4, Table 2). Here, data for the initial

supports is not presented, however, our previous investigation showed that the increasing of Zr content within Ce-Zr mixed oxides leads to an increase in the reducibility of these materials with reduction starting just above 550 K [4]. In case of both pure copper modifications the main reduction effect starts at very low temperatures (below 400 K) which could be ascribed to the reduction of very finely and narrowly dispersed CuO particles (Fig. 4, Table 2) because they undergo a complete reduction within relatively narrow temperature interval (380 – 450 K).

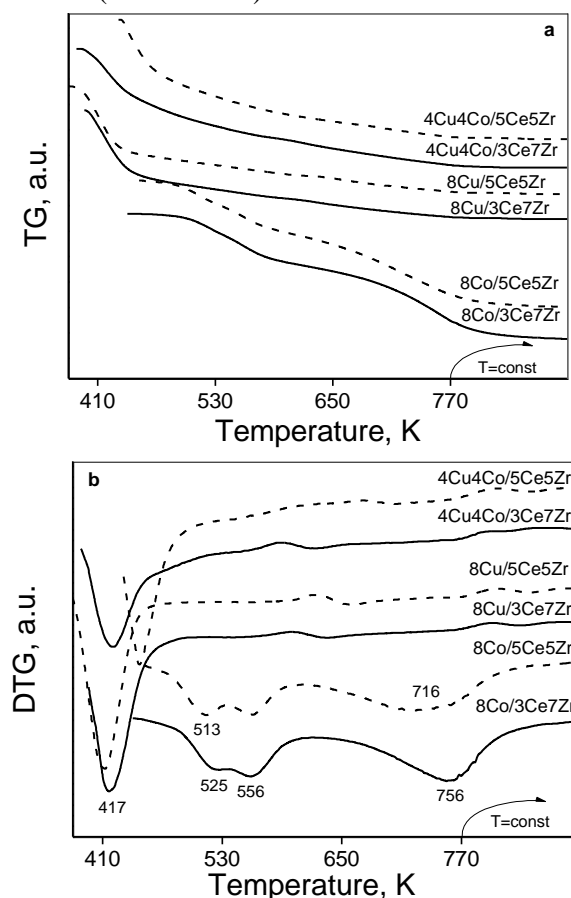


Fig. 4. TG (a) and DTG (b) data for the studied Cu and/or Co modifications.

The observed effects above 450 K could be ascribed to the reduction of Ce-Zr support which is facilitated by the reduced copper phase. In case of pure cobalt modifications, the reduction initiates at 460–470 K and stepwise reduction of Co^{3+} first to $Co^{2.5+}$ then to Co^{2+} and finally to Co^0 occurs (Fig. 4b). The observed overall weight loss corresponds to slightly less than 100 % reduction. In accordance with the XRD and UV-Vis data, this could be due to the reduction of a mixture of Co_2O_3 and Co_3O_4 phase. It should be noted the certain

shift of the reduction effects to lower temperatures in case of 5Ce5Zr cobalt modification, which could be a result of enhanced Co-Ce interactions due to higher cerium amount in this sample.

Table 2. TPR data for the obtained copper and/or cobalt modifications.

Sample	Tini, K	Tmax, K	Total weight loss, mg	Reduction degree, %
8Cu/3Ce7Zr	395	417	1.08	134
8Cu/5Ce5Zr	380	412	1.06	132
4Cu4Co/3Ce7Zr	388	420	1.16	110
4Cu4Co/5Ce5Zr	430	446	1.17	111
8Co/3Ce7Zr	470	525; 557; 756	1.22	94
8Co/5Ce5Zr	462	513; 556; 716	1.24	95

*The reduction degree is calculated on the basis of theoretic calculations for $\text{Cu}^{2+} \rightarrow \text{Cu}^0$ reduction in the case of copper modifications, $\text{Co}^{3+} \rightarrow \text{Co}^0$ reduction for the cobalt modifications and both $\text{Cu}^{2+} \rightarrow \text{Cu}^0$ and $\text{Co}^{3+} \rightarrow \text{Co}^0$ reduction transitions for Cu-Co bicomponent modifications.

According to the literature [20] cobalt cations modify the surface oxygen vacancy of ceria at the atomic level and well defined reactive faces are exposed between the interface of ceria host and the cobalt oxide. The mixed Cu-Co modifications show only one well defined effect at lower temperatures (Fig. 4, Table 2) followed by a broad tail that could be ascribed to the reduction of copper-cobalt spinel phase. The found higher than the theoretical degrees of reduction for both samples (Table 2) are an indication of facilitated reduction of the Ce-Zr supports as in the case of the pure copper modifications. The catalytic properties of the modified samples were studied in temperature-

programmed regime within the range of 423–773 K (Fig. 5). For comparison are presented data for the pure Ce-Zr mixed oxide supports calcined at 773 K as the obtained modifications. The results clearly show that the introduction of copper and/or cobalt (8 wt. % in total) within the parent Ce-Zr nanomaterial could decrease the start of the conversion with up to 50 K, leads to a substantial increase in the catalytic activity within the 550–650 K range and to almost complete selectivity to total oxidation of ethyl acetate in the whole studied temperature interval in comparison with the pure Ce-Zr supports (Figure 5a, and b). We ascribe these findings to the significantly improved redox function of the catalysts, especially at low conversion temperatures. The influence of the type of modifying transition metal is better distinguished for the 3Ce7Zr support, especially within 550–600 K range, and the results show that the presence of copper has a higher beneficial effect on the catalytic activity than cobalt (Fig. 5). At the same time, in case of all 5Ce5Zr modifications the conversion curves are very similar and close to the best results found for 8Cu/3Ce7Zr (Fig. 5a) most probably due to the higher ceria content within them, which in case of cobalt containing modifications is very beneficial as Co-Ce interactions induce the exposure of well-defined reactive faces between ceria and cobalt oxide interface [20]. On the basis of the latter results we could conclude that the presence of copper oxide particles in very highly dispersed state is of primary significance for the studied reaction. Similar findings we have already observed for nanocomposite catalysts containing nanosized Cu-Ce oxides supported on various porous silica materials [21].

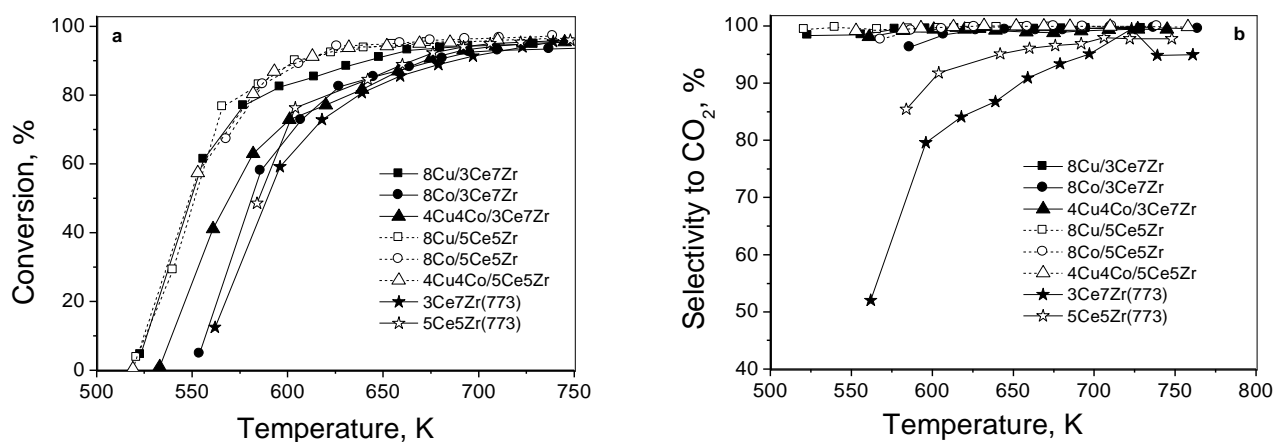


Fig 5. Temperature dependency of ethyl acetate oxidation for the studied samples.

CONCLUSION

By using a simple incipient wetness impregnation technique we could introduce and stabilize very finely dispersed copper oxide particles preferably within the micropores of nanosized mixed Ce-Zr oxides with micro-/mesoporous structure. The close contact of the obtained copper oxide species with the support structure improves substantially the overall redox properties of the obtained nanocomposites, especially at low temperatures (below 550 K), which is of primary importance for their ability to decrease the start of the conversion with about 50 K and to almost completely oxidize ethyl acetate to CO₂ even at low conversion rates and temperatures in comparison with the pure Ce-Zr nanomaterials. On the other hand, the introduction of cobalt- or copper-cobalt oxide phase leads to its deposition preferably within the smaller support mesopores (2-4 nm) and/or on the outer surface (in the case of pure cobalt modifications) which leads to a decrease in the catalytic activity for 4Cu4Co/3Ce7Zr and 8Co/3Ce7Zr modifications in comparison with 8Cu/3Ce7Zr. At the same time all 5Ce5Zr modifications show very close catalytic behavior similar to that of 8Cu/3Ce7Zr, which make these materials very perspective as catalysts for the total oxidation of ethylacetate and also other volatile organic compounds.

Acknowledgements: Financial support by Program for career development of young scientists, BAS (project DFNP 145 /12.05.2016) is gratefully acknowledged

REFERENCES

1. J. R. Salge, B. J. Dreyer, P. J. Dauenhauer, L. D. Schmidt, *Science*, **314**, 801 (2006).
2. W. Ruettinger, X. S. Liu, R. J. Farrauto, *Appl. Catal., B*, **65**, 135 (2006).
3. S. McIntosh, R. J. Gorte, *Chem. Rev.*, **104**, 4845 (2004).
4. R. N. Ivanova, M. D. Dimitrov, D. G. Kovacheva, T. S. Tsoncheva, *Bulg. Chem. Commun.*, **48-G**, 125 (2016).
5. R. N. Ivanova, M. D. Dimitrov, D. G. Kovacheva, T. S. Tsoncheva, *Bulg. Chem. Commun.*, **49-A**, 84 (2017).
6. P.-O. Larsson, A. Andersson, *Appl. Catal., B*, **24**, 175 (2000).
7. A. R. Gandhe, J. S. Rebelló, J. L. Figueiredo, J. B. Fernandes, *Appl. Catal., B*, **72**, 129 (2007).
8. P. Fang, J. Lu, X. Xiao, M. Luo, *J. Rare Earth*, **26**, 250 (2008).
9. M. Dimitrov, R. Ivanova, N. Velinov, J. Henych, M. Slušná, V. Štengl, I. Mitov, T. Tsoncheva, *Nano-Structures and Nano-Objects*, **7**, 56 (2016).
10. R. Prasad, G. Rattan, *Bull. Chem. React. Eng. Catal.*, **5**, 7 (2010).
11. H. Zhu, L. Dong, Y. Chen, *J. Coll. Int. Sci.*, **357**, 497 (2011).
12. H. Chen, A. Yin, X. Guo, W.-L. Dai, K.-N. Fan, *Catal. Lett.*, **131**, 632 (2009).
13. T. Tsoncheva, I. Genova, M. Dimitrov, E. Sarcadi-Priboczki, A. M. Venezia, D. Kovacheva, N. Scotti, V. dal Santo, *Appl. Catal., B*, **165**, 599 (2015).
14. M. Manzoli, R. Di Monte, F. Boccuzzi, S. Coluccia, J. Kašpar, *Appl. Catal., B*, **61**, 192 (2005).
15. Z. Zhao, R. Jin, T. Bao, X. Lin, G. Wang, *Appl. Catal., B*, **110**, 154 (2011).
16. X. Weng, J. Zhang, Z. Wu, Y. Liu, *Catal. Today*, **175**, 386 (2011).
17. J. Huang, Y. Kang, L. Wang, T. Yang, Y. Wang, S. Wang, *Catal. Commun.*, **15**, 41 (2011).
18. J. Hao, J. Wang, Q. Wang, Y. Yu, S. Cai, F. Zhao, *Appl. Catal., A*, **368**, 29 (2009).
19. T. S. Tsoncheva, I. G. Genova, N. Scotti, M. D. Dimitrov, A. Gallo, D. G. Kovacheva, N. Ravasio, *Bulg. Chem. Commun.*, **47**, 283 (2015).
20. N. Qiu, J. Zhang, Z. Wu, *Phys. Chem. Chem. Phys.*, **16**, 22659 (2014).
21. T. Tsoncheva, G. Issa, J. M. López Nieto, T. Blasco, P. Concepcion, M. Dimitrov, G. Atanasova, D. Kovacheva, *Micropor. Mesopor. Mater.*, **180**, 156 (2013).

МОДИФИЦИРАНИ С МЕД И/ИЛИ КОБАЛТ НАНОСТРУКТУРИРАНИ Ce-Zr СМЕСЕНИ ОКСИДИ КАТО ЕФЕКТИВНИ КАТАЛИЗАТОРИ ЗА ПЪЛНО ОКИСЛЕНИЕ НА ЕТИЛАЦЕТАТ

Р. Н. Иванова^{1*}, М. Д. Димитров¹, Д. Г. Ковачева², Т. С. Цончева¹

¹ *Институт по органична химия с Център по фитохимия, Българска академия на науките, 1113 София, България,*

² *Институт по обща и неорганична химия, Българска академия на науките, 1113 София, България*

Постъпила на 13 април 2017 г.; Коригирана на 15 май 2017 г

(Резюме)

Чрез използването на оригинален подход, включващ участието на уреа като утайтел и последваща хидротермална обработка, бяха получени два наноструктурирани Ce-Zr смесени оксиди с различно отношение на метала в тях (3:7 и 5:5), които впоследствие бяха модифицирани с мед и/или кобалт посредством метод на омокряне с воден разтвор на съответните метални нитрати. Получените материали бяха характеризирани с помощта на прахова рентгенова дифракция, физична адсорбция на азот, UV-Vis спектроскопия, температурно-програмирана редукция с водород, а тяхната каталитична активност и селективност беше изследвана в реакцията на окисление на етилацетат. Въвеждането на допълнителен преходен метален оксид в изходните Ce-Zr наноматериали води до намаление на началната температура на превръщане на етилацетат с до 50 K, увеличава съществено каталитичната активност в интервала 550-650 K и дава почти пълно окисление на етилацетат в цялата изследвана температурна област. Влиянието на вида на използвания преходен метал може да бъде по-добре разграничена при 3Ce7Zr носителя, особено в интервала 550-600 K, като резултатите показват, че добавянето единствено на мед е достатъчно за постигане на най-добрите каталитични резултати. Същевременно, носителят с по-високо съдържание на церий (5Ce5Zr) благоприятства каталитичното поведение и на Co-съдържащите образци, поради подобро взаимодействие Co-Ce.